5D SIMULATION STUDY OF SUPRATHERMAL ELECTRON TRANSPORT IN NON-AXISYMMETRIC PLASMAS

S. MURAKAMI, U. GASPARINO[†], H. IDEI, S. KUBO, H. MAASSBERG[†],
N. MARUSHCHENKO[‡], N. NAKAJIMA, M. ROMÉ[†*] and M. OKAMOTO

National Institute for Fusion Science, 322-6 Oroshi, Toki 509-5292, Japan
[†]*Max-Planck-Institut für Plasmaphysik, EURATOM Ass., D-85748 Garching, Germany*
[‡]*Institute of Plasma Physics, NSC-KhPTI, 310108 Kharkov, Ukraine*

Abstract

ECRH-driven transport of suprathermal electrons is studied in non-axisymmetric plasmas using a new Monte Carlo simulation technique in 5D phase space. Two different phases of the ECRH-driven transport of suprathermal electrons can be seen; one is a rapid convective phase due to the direct radial motion of trapped electrons and the other is a slower phase due to the collisional transport. The important role of the radial transport of suprathermal electrons in the broadening of the ECRH deposition profile is clarified in W7-AS. The ECRH driven flux is also evaluated and put in relation with the "electron root" feature recently observed in W7-AS. It is found that, at low collisionalities, the ECRH driven flux due to the suprathermal electrons can play a dominant role in the condition of ambipolarity and, thus, the observed "electron root" feature in W7-AS is thought to be driven by the radial (convective) flux of ECRH generated suprathermal electrons. The possible scenario of this "ECRH-driven electron root" is considered in the LHD plasma.

1. INTRODUCTION

In non-axisymmetric devices the particles trapped in the helical ripple tend to drift away from the starting magnetic surface. Thus, at low collisionalities, the suprathermal electrons generated by the electron cyclotron resonance heating (ECRH) can drift radially before being collisionally thermalized. These fast radial motions would enhance the convective transport of suprathermal electrons. The ECRH experimental results in CHS, H-E, and W7-AS have suggested the important role of the suprathermal electrons transport in the broadening of ECRH power deposition profiles[1] and in the flattening of density profiles[2]. Also the ECRH driven suprathermal electron flux is considered to play a dominant role in the recently found "electron root" feature at W7-AS[3, 4], where a strongly positive radial electric field, E_r (≥ 40kV/m), and a reduction of thermal diffusivity have been measured. These facts have put a considerable interest in a quantitative analysis of the ECRH driven transport due to the drift motion of suprathermal electrons. However, because of the non-local nature of the suprathermal electron transport, conventional local approaches can not be utilized for this analysis.

In this paper we study the ECRH driven transport of suprathermal electrons in non-axisymmetric plasmas solving the drift kinetic equation as a (time-dependent) initial value problem based on the Monte Carlo technique (in 5D phase space)[5, 6]. A technique similar to the adjoint equation for dynamic linearized problems is used and the linearized drift kinetic equation for the deviation from the Maxwellian background, δf, is solved. In the linearized kinetic equation, the wave-induced flux in velocity space (quasi-linear diffusion term) is obtained from 3D ray-tracing calculations and the steady-state distribution function is evaluated through a convolution with a characteristic time dependent "Green's function".

---

[*]Present address: INFM and Dipartimento di Fisica, Universitá degli Studi di Milano, Milano, Italy

In the following we explain the simulation model and our new Monte Carlo simulation code in Sec. 2. In Sec. 3 the behaviour of the ECRH generated suprathermal electrons is analyzed and the effect of ECRH-driven transport on the ECRH power deposition profile are investigated in the W7-AS plasma. In Sec. 4 the relation between the ECRH-driven electron flux and the experimentally observed "electron root" feature in W7-AS is studied and the possible scenario of similar "electron root" feature experiment is considered in the LHD plasma. The conclusions are given in Sec. 5.

2. SIMULATION MODEL

Because of the non-local nature of the ECRH-driven transport in stellarators we must consider the electron distribution function at least in five dimensional phase space. We solve the drift kinetic equation as a (time-dependent) initial value problem based on the Monte Carlo technique.

Writing the gyrophase averaged electron distribution function as

$$f(\boldsymbol{x}, v_\parallel, v_\perp, t) = f_{Max}(r, v^2) + \delta f(\boldsymbol{x}, v_\parallel, v_\perp, t),$$

where $f_{Max}(r, v^2)$ represents the Maxwellian only depending on the effective radius, r, via $n_e(r)$ and $T_e(r)$ the drift kinetic equation can be reformulated with the initial condition $\delta f(\boldsymbol{x}, v_\parallel, v_\perp, t = 0) = 0$:

$$\frac{\partial \delta f}{\partial t} + (\boldsymbol{v}_d + \boldsymbol{v}_\parallel) \cdot \frac{\partial \delta f}{\partial \boldsymbol{x}} + \dot{\boldsymbol{v}} \cdot \frac{\partial \delta f}{\partial \boldsymbol{v}} - C^{coll}(\delta f) = S^{ql}(f_{Max}), \tag{1}$$

where $\boldsymbol{v}_d$ is the drift velocity and $\boldsymbol{v}_\parallel (= v_\parallel \hat{\boldsymbol{b}})$ is the parallel velocity, respectively. The acceleration term $\dot{\boldsymbol{v}} = (\dot{v}_\parallel, \dot{v}_\perp)$ is given by the conservation of magnetic moment $\partial \mu / \partial t = 0$ and total energy $\partial E / \partial t = 0$ ($\dot{v}_\parallel = -(q/mB) \boldsymbol{B} \cdot \boldsymbol{\nabla}\Phi - (v_\perp^2/2B^2) \boldsymbol{B} \cdot \boldsymbol{\nabla}B + (v_\parallel/B^3)(\boldsymbol{B} \times \boldsymbol{\nabla}\Phi) \cdot \boldsymbol{\nabla}B$ and $\dot{v}_\perp = (v_\perp v_\parallel/2B^2) \boldsymbol{B} \cdot \boldsymbol{\nabla}B + (v_\perp/2B^3)(\boldsymbol{B} \times \boldsymbol{\nabla}\Phi) \cdot \boldsymbol{\nabla}B)$, and C^{coll} and S^{ql} are the collision operator and the quasi-linear diffusion operator for the absorption of the ECRH power, respectively. Here the quasi-linear effects, $S^{ql}(\delta f)$, is not included in the quasi-linear source term and the linear collision operator is assumed for simplicity.

It is convenient to introduce the Green function $\mathcal{G}(\boldsymbol{x}, v_\parallel, v_\perp, t \mid \boldsymbol{x}', v_\parallel', v_\perp')$ which is defined by the homogeneous Fokker-Planck equation corresponding to eq. (1).

$$\frac{\partial \mathcal{G}}{\partial t} + (\boldsymbol{v}_d + \boldsymbol{v}_\parallel) \cdot \frac{\partial \mathcal{G}}{\partial \boldsymbol{x}} + \dot{\boldsymbol{v}} \cdot \frac{\partial \mathcal{G}}{\partial \boldsymbol{v}} - C^{coll}(\mathcal{G}) = 0 \tag{2}$$

with the initial condition

$$\mathcal{G}(\boldsymbol{x}, v_\parallel, v_\perp, t = 0 \mid \boldsymbol{x}', v_\parallel', v_\perp') = \delta(\boldsymbol{x} - \boldsymbol{x}')\,\delta(\boldsymbol{v} - \boldsymbol{v}'). \tag{3}$$

The Green function, $\mathcal{G}$, has a straight-forward physical interpretation[7,8]. An electron starting at the time $t = 0$ at the position $\boldsymbol{x}'$ with the velocity $\boldsymbol{v}'$ will be found with the probability $\mathcal{G}(\boldsymbol{x}, v_\parallel, v_\perp, t \mid \boldsymbol{x}', v_\parallel', v_\perp')\, d\boldsymbol{x}\, d\boldsymbol{v}$ at the time t in the phase space volume element $d\boldsymbol{x}\, d\boldsymbol{v}$ centered at $\boldsymbol{x}$, $\boldsymbol{v}$. Then, the solution of the inhomogeneous problem of eq. (1), δf, is given by the convolution with $\mathcal{G}$:

$$\delta f(\boldsymbol{x}, \boldsymbol{v}, t) = \int_0^t dt' \int d\boldsymbol{x}' \int d\boldsymbol{v}'\, S^{ql}(f_{Max}(r', v'^2))\, \mathcal{G}(\boldsymbol{x}, \boldsymbol{v}, t - t' \mid \boldsymbol{x}', \boldsymbol{v}'). \tag{4}$$

In the quasi-linear source term $S^{ql}(f_{Max})[= -\frac{\partial}{\partial \boldsymbol{v}}(\boldsymbol{D}^{ql} \cdot \frac{\partial f_{Max}}{\partial \boldsymbol{v}})]$, the quasi-linear diffusion operator is defined with respect to $\boldsymbol{D}^{ql}(\boldsymbol{x}', \boldsymbol{v}', t')$. For stationary conditions, this explicit time-dependence in $\boldsymbol{D}^{ql}$ disappears, and the integration is performed in the limit $t \to \infty$. In this approach, only the Green function $\mathcal{G}$ has to be determined by the Monte Carlo technique.

The Green function approach has been implemented in the Monte Carlo simulation code[9,10]. The code allows for the calculation of the drift orbits with high accuracy in a complex magnetic field

configuration solving the equation of motions in the Boozer magnetic coordinates[11] based on a three dimensional MHD equilibrium. The collisional effects (both pitch angle and energy scattering) are taken into account using the linear Monte Carlo collision operator[12].

The presented solution refers to the linear ECRH problem, where the effect of the quasi-linear deformation of the distribution function on the absorption processes itself is disregarded. In this approximation, the obtained δf is therefore proportional to the injected power. Also for simplicity, the densities and temperatures of background plasma were assumed to be radially constant.

The quasi-linear diffusion term is evaluated by means of a 3D Hamiltonian ray-tracing code. This code makes use of the quasi-linear expression in the limit of a homogeneous magnetic field[13], and $D^{ql}_{\perp\perp}$ is evaluated by overlapping the contributions from several discrete rays. Whereas the r, $v_\parallel$, $v_\perp$ dependence of $D^{ql}_{\perp\perp}$ is very sensitive to the absorption mechanism, the dependence on both the toroidal and poloidal angle mainly reflects the ECRH beam width.

3. SUPRATHERMAL ELECTRON BEHAVIOR AND ECRH DEPOSITION PROFILE

We first study the behavior of suprathermal electrons and the effect on the broadening of ECRH deposition profile in W7-AS plasma (standard configuration). The quasi-linear source term for ECRH in the W7-AS configuration is evaluated by a 3D ray-tracing code and, then, the linearized drift kinetic equation is solved. Figure 1-(a) shows the time development of radial profile of $\Delta\langle\delta f^+\rangle/\Delta t(r,t) = \langle\int d\boldsymbol{v}'\int d\boldsymbol{x}'\mathcal{G}\cdot S^{ql+}\rangle$ (S^{ql+} is the positive part of S^{ql} and $\langle\rangle$ means the flux surface average) which shows the radial diffusion of suprathermal electrons generated by ECRH (X-mode 2nd harmonic). In this plot the time means the past time from the generation of the suprathermal electrons by ECRH. We set the plasma parameters as $n_0 = 1.0 \times 10^{19}$cm^{-3}, $T_e = 2.6$ keV, $T_i = 0.5$keV, $Z_{eff} = 2$ and $B_0 = 2.5$T, respectively. We can see that the radial profile rapidly extends to outside during the first 0.1msec and, then, gradually broadens. It is also found that the lower distribution of $\Delta\langle\delta f^+\rangle/\Delta t$ moves faster than higher one.

In order to see more clearly the diffusion of the suprathermal electrons we define the quantity w_d which is the radial width of $\Delta\langle\delta f^+\rangle/\Delta t$ with a specified value. In Fig. 1-(b) we show the time history of w_d for two values of $\Delta\langle\delta f^+\rangle/\Delta t$; $\Delta\langle\delta f^+\rangle/\Delta t = 1$ and 3×10^{14}cm^{-3}sec^{-1}. It is found that the broadening in the radial direction can be separated into two different phases, namely, a first rapid phase (till 0.1msec) and a second slower phase (after 0.1msec). The first period of the phase is shorter than the slowing down time of the typical suprathermal electrons ($\sim 10keV$). The broadening speed of the first phase is about 3×10^5 cm/sec in the case of $\Delta\langle\delta f^+\rangle/\Delta t = 1 \times 10^{14}$cm^{-3}sec^{-1}. This value is of the same order as the
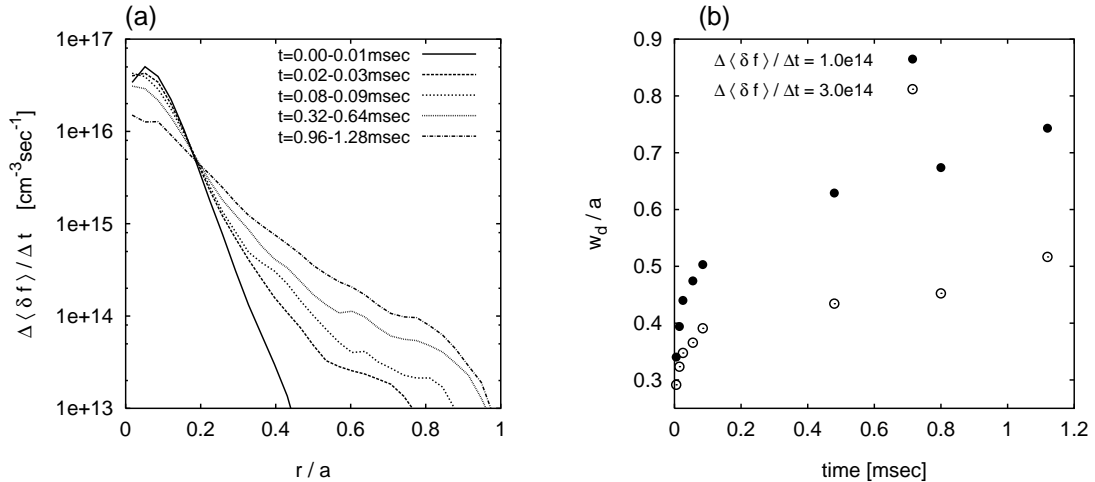

FIG. 1. Time development of the radial distribution of suprathermal electrons generated by ECRH; (a) radial profile of $\Delta\langle\delta f^+\rangle/\Delta t$ and (b) time history of w_d (the radial width of $\Delta\langle\delta f^+\rangle/\Delta t$).
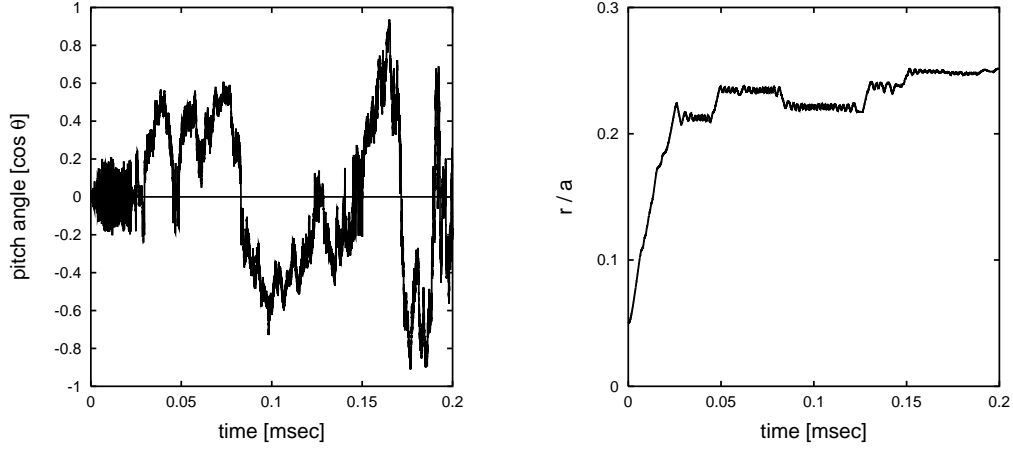
FIG. 2. Time history of the pitch angle and averaged radial position of a test suprathermal electron with a initial energy of 10 keV. The collisional time for this electron is about 0.36msec. [$T_0 = 2$ keV, $n_0 = 2.0 \times 10^{13}$cm^{-3}].
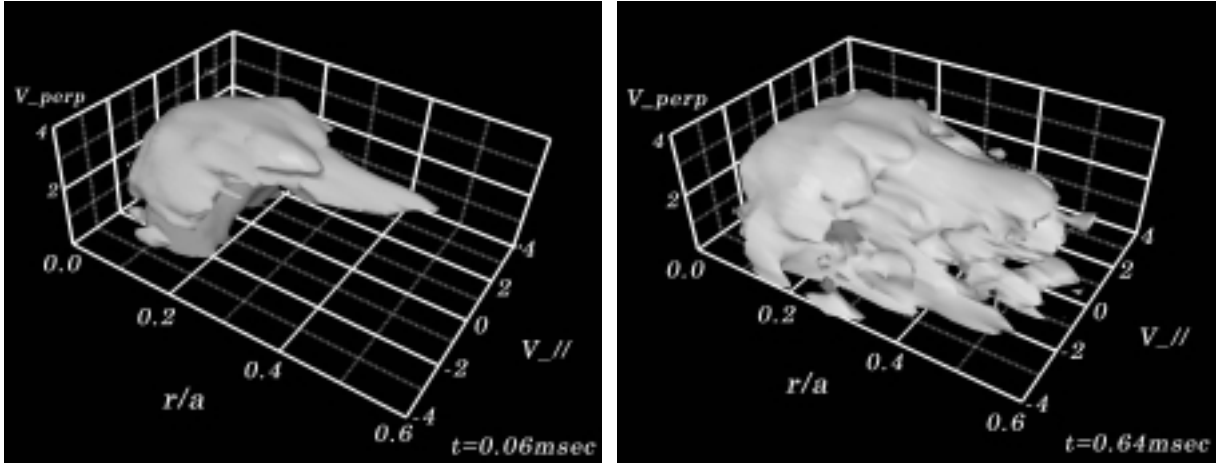

FIG. 3. Isosurface plots of the distribution δf (the deviation from the Maxwellian driven by ECRH).

radial drift velocity of typical suprathermal electrons. So we can say that the first phase is related to the direct convective transport of the radial drift of trapped electrons. On the other hand, the broadening speed of second phase in the same case is about 2.4×10^3cm/sec and the second phase would be related to the collisional transport.

To study the two time scale of the suprathermal electron transport we analyze the (collisional) orbit of a test suprathermal electron in W7-AS (standard magnetic field configuration) and study the radial motion of suprathermal electrons. Figure 2 shows the time history of the pitch angle and averaged radial position of a typical suprathermal electron born in the ECRH launching plane with an initial energy of 10 keV. As time passes, the electron energy is slowed down and the pitch angle scattered by Coulomb collisions. The fast oscillations of the pitch angle across the zero line indicate that the test electron has become trapped. One can see that the test electron directly drift radially during first 0.05msec as trapped particle. Then, after this time, the radial drift occurs when trapped due to the pitch angle scattering. Therefore it is found that the first rapid phase of radial extension is due to the convective transport of trapped suprathermal electrons and the second slow phase is due to the collisional transport.

We can also see the difference of these two phases in the distribution of δf. Figure 3 shows the
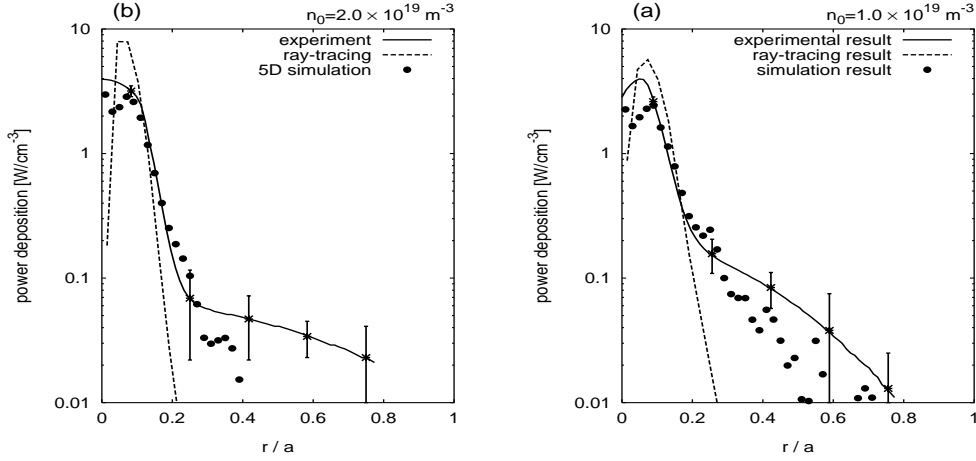
4

FIG. 4. Comparisons of the simulation results of ECRH deposition profile ($\bullet$) with the ray-tracing (dashed line) and experimental ones[1] (solid line) for two different plasma parameters; (a) $n_0 = 2.0 \times 10^{19}$cm^{-3} and $T_e = 2.2$ keV, and (b) $n_0 = 1.0 \times 10^{19}$cm^{-3} and $T_e = 2.6$ keV.

isosurface plots of (magnetic surface averaged) δf in the three dimensional space ($v_\perp$, $v_{//}$, r) at the two different times, $t = 0.06$ and 0.64msec. In the figure the lower (upper) surfaces show the negative (positive) regions of δf, respectively. ECRH tends to push resonant electrons towards higher energies, consequently a depletion (with respect to the Maxwellian) tends to appear at lower energies and a tail at higher energies. We can see a "nose-like structure" at the upper surface which is related to the radial convective transport of the energetic trapped particles at $t = 0.06$msec. Then, the suprathermal electrons start to slow-down and the radial diffusion occurs uniformly in the velocity space (we can not see a clear "nose-like structure").

Using the obtained distribution δf, we can evaluate the ECRH deposition profile. Figure 4 shows the comparison of the simulation results of ECRH deposition profile ($\bullet$) with the ray-tracing (dashed line) and experimental ones (solid line) for X-mode 2nd-harmonic ECRH in the standard configuration [1]. The plasma parameters are (a) $n_0 = 2.0 \times 10^{19}$cm^{-3} and $T_e = 2.2$ keV, and (b) $n_0 = 1.0 \times 10^{19}$cm^{-3} and $T_e = 2.6$ keV. The other parameters are fixed to $B_0 = 2.5$T, $T_i = 0.5$keV, and $Z_{eff} = 2$. It is found that the broader deposition profile from the ray-tracing prediction is obtained in both cases and the larger broadening can be seen in the lower collision frequency case (b). We can see a relatively good agreement between the experimental and numerical results for both cases. This tends to confirm the important role of radial convective transport of suprathermal electrons in the broadening of ECRH deposition profile in W7-AS.

4. ECRH-DRIVEN "ELECTRON ROOT"

The neoclassical "electron root" feature has been observed in W7-AS. A strongly positive radial electric field, E_r, ($\geq$ 40kV/m) has been measured in the central plasma region in W7-AS and the experimental heat diffusivity becomes much lower than the neoclassical one for $E_r \simeq 0$, leading to highly peaked central electron temperatures (up to 6 keV). These results agree to the "electron root" features of the neoclassical theory. However, there are also disagreement points with the neoclassical predictions. One thing is the smaller reduction of heat diffusivity than that estimated by neoclassical theory and the other is the strong relation to ECRH (injection mode and configuration at launching plane). These disagreement points and experimental ECE measurements strongly suggest a connection between the "electron root" feature and the ECRH-driven flux. We consider here the effect of ECRH-driven flux on the ambipolar conditions in relation with the "electron root" experiments at W7-AS.
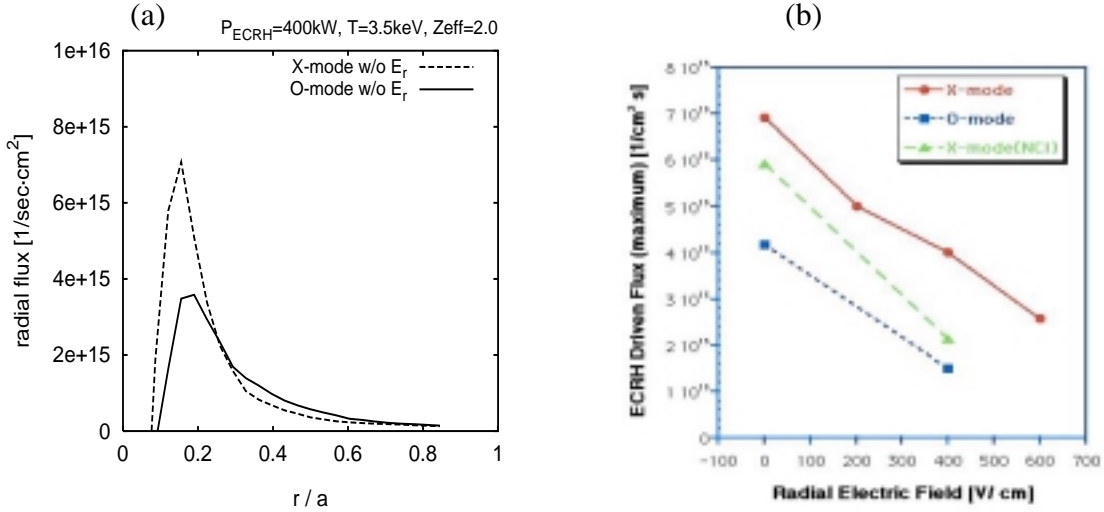
5

FIG. 5. ECRH driven electron flux. (a) comparison of the radial profile for X- and O-mode cases, and (b) E_r dependencies of the maximum value of the driven flux.

The "electron root" feature was only observed in low density discharges with high power ($\geq$ 400k-W) X-mode 2nd-harmonic ECRH and, up to now, could not be driven by O-mode 1st-harmonic. We, first, evaluate the ECRH-driven flux by suprathermal electrons to show the difference between these two polarizations. Figure 5-(a) shows the simulations of the radial profile of the ECRH driven electron flux for the two polarizations. It is found that the large ECRH-driven fluxes are obtained for both cases in the central plasma region ($r/a \sim 0.2$) where the "electron root" feature has been observed, and that the flux for the X-mode case ($\sim 7 \times 10^{15} \mathrm{sec}^{-1} \cdot \mathrm{cm}^{-2}$) is about 2 times higher than that for O-mode ($\sim 4 \times 10^{15} \mathrm{sec}^{-1} \cdot \mathrm{cm}^{-2}$) at maximum points. This is related to the different absorption mechanism for the two polarizations. The X-mode is mainly absorbed by deeply trapped particles (maximum of absorption by resonant electrons with $v_{//} \simeq 0$), while the absorption for perpendicularly injected O-mode, requiring finite values of $v_{//}$, is shifted towards the passing particle region [1].

Also we evaluated the ECRH-driven flux under a strongly positive E_r assuming a similar E_r profile as the experimentally observed one. The E_r dependency of the maximum value of the ECRH driven flux is shown in Fig. 5-(b) for the standard configuration (two polarizations) and for a "low mirror" configuration without trapped electrons in the ECRH launching plane (X-mode). The largest electron flux is found in the case of X-mode for the standard configuration which is the case the "electron root" feature is only observed with the 400kW of ECRH heating power. Interestingly, the E_r dependency seems to be weaker than that of the neoclassical flux which is proportional to $E_r^{-3/2}$. This is because the radial transport of suprathermal electron mainly caused by the direct convective motion of trapped electrons. These results suggests the important role of ECRH-driven flux in the "electron root" feature.

Figure 6 shows the comparison of the ECRH driven flux and the ambipolar neoclassical fluxes obtained by the DKES code. The solid lines show the X-mode ECRH driven flux without E_r evaluated by our simulation code. The full and dashed lines show the X-mode ECRH driven flux for the case without and with a strong positive E_r($\sim$ 400V/cm), respectively. The circles refers to the DKES results. We can see that the ECRH driven flux is comparable to the ambipolar neoclassical thermal one with the ion root ($E_r \sim 0$) and much larger than the ambipolar neoclassical thermal one with strongly positive E_r region. These suggest that the ECRH-driven flux plays dominant role to drive strongly positive E_r and, therefore, we can conclude that the experimentally observed "electron root" in W7-AS is driven by the radial flux of ECRH generated suprathermal electrons.

We, next, consider the possible scenario of this "ECRH-driven electron root" in the LHD plasma. As shown in Fig. 6, the "ECRH-driven electron root" could be expected when the ECRH driven flux,
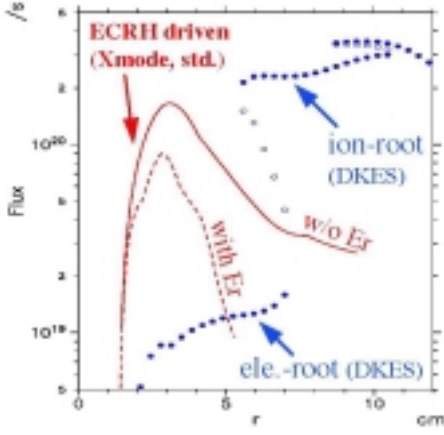
6

FIG. 6. Comparisons of the simulation results of the ECRH driven fluxes with total background plasma fluxes in W7-AS.
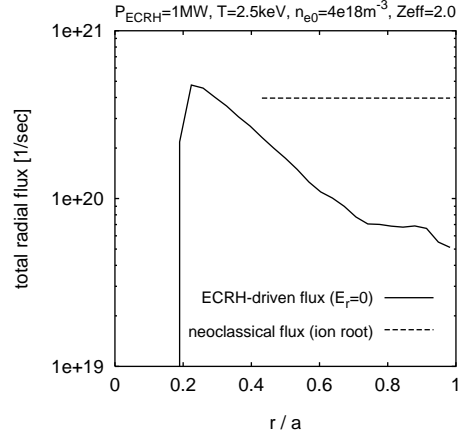

FIG. 7. Comparisons of the simulation results of the ECRH driven flux with the total background plasma flux in LHD.

Γ^{ECRH}, is comparable with background neoclassical flux, Γ^{NC}. In order to obtain such a large Γ^{ECRH} we need a sufficiently big fraction of trapped suprathermal electrons. So we assume the LHD magnetic configurations with $\Delta_{ax} = 0$cm (0cm shift of magnetic axis from the coil center). And the heating point is selected as $r/a \sim 0.2$. Also we assume 1MW of heating power and the plasma parameters are as follows; $n_0 = 4 \times 10^{18}$m^{-3}, $T_{e0} = 2.5$keV, $Z_{eff} = 2$ and $B_0 = 1.5$T. The background neoclassical flux can be simply written, assuming $E_r \sim 0$ ("ion root") and no density gradient, as

$$\Gamma^{NC} = \delta_D \frac{q_e}{T_e}, \tag{5}$$

where q_e and T_e are the electron heat flux and temperature, respectively, and δ_D is the ratio between D_{12}^e and D_{22}^e with D_{ij}^e the thermal transport matrix for electrons. Then, the total background neoclassical flux is evaluated as $F^{NC} = \int \Gamma^{NC} dS \simeq 4 \times 10^{20}$sec^{-1}, where the value of δ_D is assumed to be $\delta_D \sim 1/6$[14]. We evaluate the ECRH-driven flux in the LHD plasma assuming these parameters. Figure 7 shows the comparison of the ECRH-driven flux (solid line) with background neoclassical flux (dashed line) in the LHD plasma. We can see that the large ECRH-driven flux is obtained in the central plasma region and that the value of ECRH-driven flux is comparable with the ion root flux near $r/a \sim 0.2$. So we can expect that the ECRH-driven "electron root" would be observed near the central region in the LHD.

Finally we discuss the possibility of the "ECRH-driven electron root" with higher density. If we assume that the ECRH-driven flux is mainly generated by the convective flux of trapped suprathermal electrons, then, the total ECRH-driven flux at the maximum point, $F_{max}^{ECRH}(r)(= \int \Gamma^{ECRH} dS)$, can be simply written as

$$F_{max}^{ECRH} = \frac{1}{\Delta_{abs}} \int_0^{\Delta_{abs}} dl \frac{f_{tr} P_{ECRH}}{\epsilon_{se}} p_r(l) \tag{6}$$

where f_{tr}, ϵ_{se} and Δ_{abs} are the fraction of the trapped suprathermal electrons, the characteristic energy of suprathermal electrons and the width of ECRH absorption region, respectively. And $p_r(l)$ is the the probability that a suprathermal electron move radially from the generated point to the distance l and we here assume $p_r(l) = \exp(-\alpha l/l_r^{se})$, where l_r^{se} is the mean free path of suprathermal electrons in the radial direction and α is a constant. Then the necessary condition for the ECRH-driven electron root can be written as

$$\frac{F_{max}^{ECRH}}{F^{NC}} \sim \frac{f_{tr}}{\delta_D \gamma_{se}(1 - f_{tr})} \left(\frac{l_r^{se}}{\alpha \Delta_{abs}} \right) \{1 - \exp(-\alpha_l \Delta_{abs}/l_r^{se})\} \geq C, \tag{7}$$

where $\gamma_{se} = \epsilon_{se}/T_e$ and $C(\sim 1)$ is the constant. This relation shows that only l_r^{se} strongly depend on the plasma density and temperature and the other parameters mainly depends on the configurations and

ECRH conditions. Thus, l_r^{se} is a key factor which is approximately as

$$l_r^{se} \sim v_r / \nu_{se}^{eff} \propto n^{-1} \epsilon_{se} T_e^{3/2}, \tag{8}$$

where v_r and ν_{se}^{eff} are the radial drift velocity and the effective collision frequency of trapped particles, respectively. Assuming $\epsilon_{se} \propto T_e$ and the LHD scaling for energy confinement time of background plasma we obtain $l_{se} \propto n^{-1.78} P^{1.1}$. Then we can obtain the relation between the density and the threshold heating power for the "ECRH-driven electron root", P_c^{EDER}, as

$$P_c^{EDER} \propto n^{1.6}. \tag{9}$$

This relation show that we need a much higher heating power to obtain the "ECRH-driven electron root" with higher density.

5. CONCLUSIONS

The non-local transport of ECRH generated suprathermal electrons have been studied in W7-AS using a new Monte Carlo code in 5D phase space. The time development of the suprathermal electron radial profile and the orbit analysis clearly show two different phases in the ECRH-driven transport. One is a rapid convective phase due to the direct radial motion of trapped electrons and the other is a slower phase due to the collisional transport. The distribution δf also shows the important role of trapped suprathermal electrons in the radial (convective) transport driven by the ECRH. The simulated broadening of the ECRH deposition profile is found to be in relatively good agreement with the experimentally inferred one.

The code was also applied to evaluate the ECRH driven flux in the "electron root" experiments at W7-AS. Simulation results show that in the central plasma region X-mode 2nd-harmonic ECRH is more "efficient" than O-mode 1nd-harmonic in driving radial electron fluxes. This could explain why the "electron root" (and the related improvement of confinement) was experimentally found only for X-mode. Comparisons with neoclassical predictions (DKES code) have shown the dominant role played by the ECRH driven flux in the ambipolarity condition for the central region where the strongly positive E_r is experimentally observed. Thus the experimentally observed "electron root" in W7-AS thought to be driven by the radial flux of ECRH generated suprathermal electrons.

The possible experimental condition for the ECRH-driven electron root has been studied in the LHD plasma. It is found that the ECRH-driven flux becomes comparable to the neoclassical background flux with ion root and the ECRH-driven electron root could be expected when we assume the outward shifted configuration of LHD ($\Delta_{ax} = 0$cm) with relatively a low density. Also we derive the relation between the threshold power for ECRH-driven electron root and the plasma density as $P_c^{EDER} \propto n^{1.6}$, which indicate that much higher heating power is necessary to obtain ECRH-driven electron root with higher density.

References

[1] ROMÉ, M., et al., Plasma Phys. Contr. Fusion **39** (1997) 117.
[2] IDEI, H., et al., Phys. Plasmas **1** (1994) 3400.
[3] MAASSBERG, H., et al., J. Plasma Fusion Res. SERIES, Vol. 1 (1998) 103.
[4] WAGNER, F, et al., these proceedings.
[5] MURAKAMI, S., et al., *Proc. 16th IAEA Fusion Energy Conf.*, Montreal, 1996, Vol. **2**, p 157.
[6] MURAKAMI, S., et al., J. Plasma Fusion Res. SERIES, Vol. 1 (1998) 122.
[7] FISH, N. J., Rev. Mod. Phys. **59** (1987) 175.
[8] RAX, J. M. and MOREAU, D., Nucl. Fusion **29** (1989) 1751.
[9] MURAKAMI, S., et al., Nucl. Fusion **34** (1994) 913.
[10] MURAKAMI, S., et al., in Plasma Physics and Controlled Nuclear Fusion Research 1994 (Proc. 15th Int. Conf. Sevilla, 1994), Vol. 3, IAEA, Vienna (1995) 531.
[11] FOWLER, R. H., et al., Phys. Fluids **28** (1985) 338.
[12] BOOZER, A. H. and KUO-PETRAVIC, G., Phys. Fluids **24** (1981) 851.
[13] KENNEL, C. F. and ENGELMANN, F, Phys. Fluids **9** (1996) 2337.
[14] MAASSBERG, H., et al., J. Plasma Fusion Res. SERIES, Vol. 1 (1998) 230.